

FILE COPY  
NO. 2-W

CASE FILE N 62 65032  
COPY

NATIONAL ADVISORY COMMITTEE FOR AERONAUTICS

# WARTIME REPORT

ORIGINALLY ISSUED  
July 1945 as  
Advance Restricted Report L5F08b

COLUMN AND PLATE COMPRESSIVE STRENGTHS

OF AIRCRAFT STRUCTURAL MATERIALS

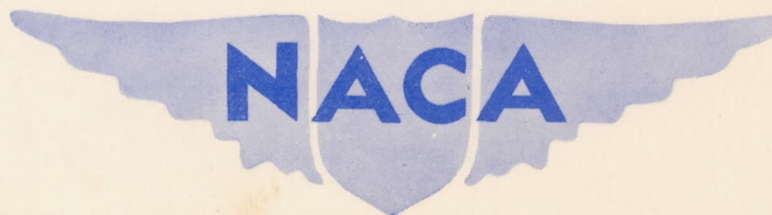
EXTRUDED 24S-T ALUMINUM ALLOY

By George J. Heimerl and J. Albert Roy

Langley Memorial Aeronautical Laboratory  
Langley Field, Va.

**FILE COPY**

To be returned to  
the files of the National  
Advisory Committee  
for Aeronautics  
Washington D. C.



WASHINGTON

NACA WARTIME REPORTS are reprints of papers originally issued to provide rapid distribution of advance research results to an authorized group requiring them for the war effort. They were previously held under a security status but are now unclassified. Some of these reports were not technically edited. All have been reproduced without change in order to expedite general distribution.

## NATIONAL ADVISORY COMMITTEE FOR AERONAUTICS

## ADVANCE RESTRICTED REPORT

COLUMN AND PLATE COMPRESSIVE STRENGTHS  
OF AIRCRAFT STRUCTURAL MATERIALS

## EXTRUDED 24S-T ALUMINUM ALLOY

By George J. Heimerl and J. Albert Roy

## SUMMARY

Column and plate compressive strengths of extruded 24S-T aluminum alloy were determined both within and beyond the elastic range from tests of thin-strip columns and local-instability tests of H-, Z-, and channel-section columns. These tests are part of an extensive research investigation to provide data on the structural strength of various aircraft materials. The results are presented in the form of curves and charts that are suitable for use in the design and analysis of aircraft structures.

## INTRODUCTION

Column and plate members in an aircraft structure are the basic elements that fail by instability. For the design of aircraft of low weight and high structural efficiency, the strength of these elements must be known for the various aircraft materials. An extensive research program has therefore been undertaken at the Langley Memorial Aeronautical Laboratory to establish the column and plate compressive strengths of a number of the alloys available for use in aircraft structures. Parts of this investigation already completed for various aluminum alloys - 24S-T sheet, 17S-T sheet, and extruded 75S-T - are given in references 1, 2, and 3, respectively.

The results of tests to determine the column and plate compressive strengths of extruded 24S-T aluminum alloy are presented herein.

## SYMBOLS

$L$	length of column
$\rho$	radius of gyration
$c$	fixity coefficient used in Euler column formula
$\frac{L}{\rho\sqrt{c}}$	effective slenderness ratio of thin-strip column
$b_F, t_F$	width and thickness, respectively, of flange of H-, Z-, or channel section (see fig. 1)
$b_W, t_W$	width and thickness, respectively, of web of H-, Z-, or channel section (see fig. 1)
$r$	corner radius (see fig. 1)
$k_W$	nondimensional coefficient used with $b_W$ and $t_W$ in plate-buckling formula (see figs. 2 and 3 and reference 4)
$E_c$	modulus of elasticity in compression, taken as 10,700 ksi for 24S-T aluminum alloy
$\tau$	nondimensional coefficient for columns (The value of $\tau$ is so determined that, when the effective modulus $\tau E_c$ is substituted for $E_c$ in the equation for elastic buckling of columns, the computed critical stress agrees with the experimentally observed value. The coefficient $\tau$ is equal to unity within the elastic range and decreases with increasing stress beyond the elastic range.)
$\eta$	nondimensional coefficient for compressed plates corresponding to $\tau$ for columns
$\mu$	Poisson's ratio, taken as 0.3 for 24S-T aluminum alloy
$\sigma_{cr}$	critical compressive stress
$\bar{\sigma}_{max}$	average compressive stress at maximum load
$\sigma_{cy}$	compressive yield stress

## METHODS OF TESTING AND ANALYSIS

All tests were made in hydraulic testing machines accurate within three-fourths of 1 percent. The methods of testing and analysis developed for this research program (reference 1) may be briefly summarized as follows:

The compressive stress-strain curves for the extrusions, which identify the material for correlation with its column and plate compressive strengths, were obtained for the with-grain direction from tests of single-thickness compression specimens cut from the extruded H-section. The tests were made in a compression fixture of the Montgomery-Templin type, which provides lateral support to the specimens through closely spaced rollers.

The column strength and the associated effective modulus were obtained for the with-grain direction by the use of the method presented in reference 5, in which thin-strip columns of the material were tested with the ends clamped in fixtures that provide a high degree of end restraint. The fixtures have been improved and the method of analysis has been modified since publication of reference 5. The method now used results in a column curve representative of nearly perfect column specimens. In addition, the method now takes into account the fact that columns of the dimensions tested are actually plates with two free edges. These columns were cut from the flanges of the H-section adjacent to the junction of the web and flange.

The plate compressive strength was obtained from compression tests of H-, Z-, and channel-section columns so proportioned as to develop local instability, that is, instability of the plate elements. (See fig. 4.) Extruded H-sections having two different web widths were tested; the flange widths for each were varied by milling off portions of the flanges. The flanges of some of the H-section extrusions were removed in such a way as to make Z- or channel sections as desired. The flange widths of the Z- and channel-section columns were varied in the same manner as the flange widths for the H-section columns. The lengths of the columns were selected in accordance with the principles of reference 6. The columns were tested with the flat ends bearing directly against the testing-machine heads. In these local-instability tests measurements were taken of the cross-sectional distortion,

and the critical stress was determined as the stress at the point near the top of the knee of the stress-distortion curve at which a marked increase in distortion first occurred with small increase in stress.

A departure from the method of analysis presented in reference 1 is that the inside face dimensions were used to define  $b_F$  and  $b_W$  in the evaluation of  $\sigma_{cr}/\eta$  by means of the equations and curves of figures 2 and 3. This definition of  $b_F$  and  $b_W$  for extruded sections with small fillets was previously used in reference 3 in order that the theoretical and experimental buckling stresses would agree within the elastic range. For formed Z- and channel sections with an inside bend radius of three times the sheet thickness (references 1 and 2),  $b_F$  and  $b_W$  were defined as center-line widths with square corners assumed.

## RESULTS AND DISCUSSION

### Compressive Stress-Strain Curves

Compressive stress-strain curves for extruded 24S-T aluminum alloy, which were selected as typical or average curves for the column material, are given in figure 5. These curves were obtained from tests of compression specimens cut from the flanges of the extrusions adjacent to the junction of the web and flanges as shown in figure 5.

In order to study the variation of the compressive properties over the cross sections, surveys were made of the extrusion by tests of compression specimens cut from the web and flanges of the H-sections. A typical variation of the compressive yield stress  $\sigma_{cy}$  over the cross section is shown in figure 6. Values of  $\sigma_{cy}$  at the outer part of the flanges are generally higher than those for the inner part of the flanges; the lowest values of  $\sigma_{cy}$  were found in the web in all cases. The stress-strain curves of figure 5, representative of the material in the flange adjacent to the web, therefore usually show conservative values of  $\sigma_{cy}$  for the flange and unconservative values of  $\sigma_{cy}$  for the web.

The columns to which a particular stress-strain curve applies are indicated in table 1 together with the value of the compressive yield stress for that stress-strain

curve. These values of  $\sigma_{cy}$  for the with-grain direction average about 50 ksi. The modulus of elasticity in compression was taken as 10,700 ksi, the present accepted value for 24S-T aluminum alloy.

### Column and Plate Compressive Strengths

Because the compressive properties of an extruded aluminum alloy may vary considerably, the data and charts of this report should not be used for design purposes for extrusions of 24S-T aluminum alloy that have appreciably different compressive properties from those obtained in these tests, unless a suitable method is devised for adjusting test results to account for variations in material properties. The results of the column and local-instability tests for extruded 24S-T aluminum alloy are summarized herein; a discussion of the basic relationships is given in reference 1.

Column strength.- The column curve of figure 7 shows the results of the thin-strip column tests for the with-grain direction. The reduction in the effective modulus of elasticity  $\tau E_c$  with increase in column stress is indicated by the variation of  $\tau$  with stress shown in figure 8.

Plate compressive strength.- The results of the local-instability tests of the H-, Z-, and channel-section columns used to determine the plate compressive strength are given in tables 2, 3, and 4, respectively. The plate-buckling curves, analogous to the column curve of figure 7, are shown in figure 9. The reduction of the effective modulus of elasticity  $\eta E_c$  with increase in stress for compressed plates is indicated by the variation of  $\eta$  with stress, which is shown along with the curve for  $\tau$  in figure 8. The crossing of the  $\tau$ - and  $\eta$ -curves shown in figure 8 occurs because the H-, Z-, and channel-section columns used to obtain the  $\eta$ -curves apparently had an appreciable degree of imperfection, which resulted in the deviation of the  $\eta$ -curves from unity at a lower stress than that at which the  $\tau$ -curve, representative of nearly perfect columns, diverges from unity.

The variation of the actual critical stress  $\sigma_{cr}$  with the theoretical critical stress  $\sigma_{cr}/\eta$  computed for elastic buckling by means of the formula and charts of figures 2 and 3 is shown in figure 10.

In order to illustrate the difference between the critical stress  $\sigma_{cr}$  and the average stress at maximum load  $\bar{\sigma}_{max}$ , the variation of  $\sigma_{cr}$  with  $\sigma_{cr}/\bar{\sigma}_{max}$  is shown in figure 11. Because values of  $\bar{\sigma}_{max}$  may be required in strength calculations, the variation of  $\bar{\sigma}_{max}$  with  $\sigma_{cr}/\eta$  is shown in figure 12.

Figures 9 to 12 show that the data for H-sections described curves different from those indicated for Z- and channel sections. One of the reasons why higher values of  $\bar{\sigma}_{max}$  were obtained for H-sections than for Z- or channel sections for a given value of  $\sigma_{cr}/\eta$  (fig. 12) may be the fact that the high-strength material in the flanges (fig. 6) forms a higher percentage of the total cross-sectional area for the H-section than for the Z- or channel section. For the H-section,  $\bar{\sigma}_{max}$  is increased over the value for the Z- or channel section over the entire stress range covered in these tests (fig. 12);  $\sigma_{cr}$  for the H-section, however, is increased only for stresses beyond the elastic range (fig. 10).

Langley Memorial Aeronautical Laboratory  
National Advisory Committee for Aeronautics  
Langley Field, Va.

1. Lundquist, Eugene E., Schuette, Evan H., Heimerl, George J., and Roy, J. Albert: Column and Plate Compressive Strengths of Aircraft Structural Materials. 24S-T Aluminum-Alloy Sheet. NACA ARR No. L5F01, 1945.
2. Heimerl, George J., and Roy, J. Albert: Column and Plate Compressive Strengths of Aircraft Structural Materials. 17S-T Aluminum-Alloy Sheet. NACA ARR No. L5F08, 1945.
3. Heimerl, George J., and Roy, J. Albert: Column and Plate Compressive Strengths of Aircraft Structural Materials. Extruded 75S-T Aluminum Alloy. NACA ARR No. L5F08a, 1945.
4. Kroll, W. D., Fisher, Gordon P., and Heimerl, George J.: Charts for Calculation of the Critical Stress for Local Instability of Columns with I-, Z-, Channel, and Rectangular-Tube Section. NACA ARR No. 3K04, 1943.
5. Lundquist, Eugene E., Rossman, Carl A., and Houbolt, John C.: A Method for Determining the Column Curve from Tests of Columns with Equal Restraints against Rotation on the Ends. NACA TN No. 903, 1943.
6. Heimerl, George J., and Roy, J. Albert: Determination of Desirable Lengths of Z- and Channel-Section Columns for Local-Instability Tests. NACA RB No. L4H10, 1944.



TABLE 1

## COMPRESSIVE PROPERTIES OF EXTRUDED 24S-T ALUMINUM ALLOY

$$[E_c = 10,700 \text{ ksi}]$$

Columns to which stress-strain curves apply		Stress-strain curve (fig. 5)	Compressive yield stress, $\sigma_{cy}$ (ksi)
Type	Designation (tables 2 to 4)		
Thin strip	All	A	50.9
H	5a, 5b, 6a, 6b, 6c, 7a, 7b, 7c, 8a, 9a, 9b	B	52.1
H	2b, 3a	C	46.1
H	1a, 1b, 1c, 2a, 2c, 3b, 3c, 4a, 4b	D	47.0
H	8b	E	52.5
Z	8	B	52.1
Z	3, 4a, 4b, 4c, 5a, 5b	C	46.1
Z	1, 2a, 2b, 2c	D	47.0
Z	9a, 9b, 10a, 10b, 10c	E	52.5
Z	6a, 6b, 6c, 7a, 7b, 7c	F	51.6
Channel	3a, 3b, 3c, 3d, 4a, 4b, 4c, 4d, 4e, 4f, 5a, 5b, 5c	C	46.1
Channel	1a, 1b, 2a, 2b	D	47.0
Channel	8a, 8b, 8c, 9a, 9b, 9c, 10a, 10b, 10c	E	52.5
Channel	6a, 6b, 6c, 7a, 7b, 7c	F	51.6

TABLE 2.- DIMENSIONS OF COLUMNS AND TEST RESULTS  
FOR EXTRUDED 24S-T H-SECTIONS

Column	$t_w$ (in.)	$t_F$ (in.)	$b_w$ (in.)	$b_F$ (in.)	L (in.)	$\frac{L}{b_w}$	$\frac{t_w}{t_F}$	$\frac{b_w}{t_w}$	$\frac{b_F}{b_w}$	$k_w$ (fig. 2)	$\frac{b_w}{t_w} \sqrt{\frac{12(1-\mu^2)}{k_w}}$	$\frac{\sigma_{cr}}{\eta}$ (ksi) (a)	$\sigma_{cr}$ (ksi)	$\bar{\sigma}_{max}$ (ksi)	$\frac{\sigma_{cr}}{\bar{\sigma}_{max}}$
1a	0.123	0.128	1.61	0.99	7.91	4.91	0.960	13.07	0.614	2.00	30.5	113.2	55.8	57.6	0.969
1b	.124	.128	1.62	.99	7.91	4.88	.965	13.09	.610	2.01	30.5	113.4	55.1	57.6	.957
1c	.124	.128	1.62	.99	7.91	4.88	.965	13.06	.610	2.01	30.4	114.0	55.1	57.3	.962
2a	.124	.128	1.61	1.09	8.76	5.44	.966	12.99	.677	1.67	33.2	95.7	52.4	55.6	.942
2b	.124	.129	1.62	1.09	8.76	5.41	.963	13.06	.673	1.69	33.2	95.8	52.7	53.8	.980
2c	.124	.128	1.61	1.09	8.74	5.43	.966	12.99	.677	1.67	33.2	95.7	51.0	54.7	.932
3a	.124	.129	1.61	1.17	9.51	5.91	.962	12.97	.727	1.48	35.3	84.8	49.9	51.1	.977
3b	.124	.128	1.61	1.17	9.66	6.00	.968	12.96	.727	1.47	35.3	84.6	50.1	51.8	.967
3c	.124	.128	1.61	1.17	9.66	6.00	.968	12.96	.727	1.47	35.3	84.6	51.8	52.4	.989
4a	.124	.128	1.61	1.34	10.85	6.74	.965	12.98	.832	1.16	39.8	66.6	46.7	47.3	.987
4b	.124	.129	1.62	1.34	10.85	6.70	.963	13.06	.827	1.17	39.9	66.3	46.7	47.5	.983
5a	.116	.120	2.76	1.10	11.49	4.16	.969	23.78	.399	3.79	40.4	64.8	47.7	48.3	.988
5b	.116	.120	2.76	1.09	11.52	4.17	.967	23.79	.395	3.83	40.1	65.4	47.0	48.7	.965
6a	.116	.120	2.76	1.38	14.39	5.21	.965	23.88	.500	2.78	47.3	47.1	42.1	43.1	.977
6b	.116	.120	2.76	1.39	14.39	5.21	.965	23.85	.504	2.75	47.5	46.8	41.7	42.6	.979
6c	.115	.120	2.75	1.39	14.39	5.23	.967	23.81	.505	2.72	47.7	46.4	41.2	42.5	.969
7a	.115	.119	2.76	1.67	15.48	5.61	.964	24.03	.605	2.05	55.4	34.3	32.6	37.2	.876
7b	.115	.119	2.75	1.67	15.49	5.63	.963	23.97	.607	2.04	55.4	34.3	33.6	36.4	.923
7c	.116	.119	2.74	1.67	15.47	5.65	.974	23.65	.609	1.99	55.4	34.4	32.3	37.2	.868
8a	.114	.119	2.74	1.97	16.64	6.07	.961	24.01	.719	1.51	64.6	25.3	25.4	35.3	.720
8b	.115	.120	2.76	1.95	16.55	6.00	.958	23.98	.707	1.56	63.4	26.2	26.6	35.6	.747
9a	.115	.120	2.74	2.24	17.84	6.51	.955	23.92	.818	1.20	72.2	20.3	20.1	33.8	.595
9b	.115	.121	2.74	2.24	17.84	6.51	.947	23.93	.818	1.22	71.6	20.6	20.1	33.8	.595

$$^a \frac{\sigma_{cr}}{\eta} = \frac{k_w \pi^2 E_c t_w^2}{12(1-\mu^2) b_w^2}, \text{ where } E_c = 10,700 \text{ ksi and } \mu = 0.3.$$

TABLE 3.- DIMENSIONS OF COLUMNS AND TEST RESULTS  
FOR EXTRUDED 24S-T Z-SECTIONS

Column	$t_w$ (in.)	$t_F$ (in.)	$b_w$ (in.)	$b_F$ (in.)	L (in.)	$\frac{L}{b_w}$	$\frac{t_w}{t_F}$	$\frac{b_w}{t_w}$	$\frac{b_F}{b_w}$	$k_w$ (fig. 3)	$\frac{b_w}{t_w} \sqrt{\frac{12(1-\mu^2)}{k_w}}$	$\frac{\sigma_{cr}}{\eta}$ (ksi) (a)	$\sigma_{cr}$ (ksi)	$\bar{\sigma}_{max}$ (ksi)	$\frac{\sigma_{cr}}{\bar{\sigma}_{max}}$
1	0.124	0.128	1.62	0.98	6.11	3.77	0.964	13.09	0.602	2.31	28.4	130.4	55.2	58.1	0.950
2a	.123	.128	1.62	1.00	6.47	3.99	.960	13.15	.615	2.24	29.0	125.3	55.0	57.0	.965
2b	.123	.128	1.62	1.00	6.46	3.99	.959	13.16	.615	2.24	29.1	125.1	54.4	56.4	.965
2c	.123	.128	1.62	1.01	7.00	4.32	.959	13.17	.623	2.20	29.3	122.7	54.1	56.5	.958
3	.126	.131	1.62	1.09	6.37	3.93	.965	12.83	.673	1.92	30.6	112.8	52.8	53.9	.980
4a	.126	.130	1.62	1.18	6.95	4.29	.966	12.86	.728	1.68	32.8	97.6	50.1	51.9	.965
4b	.124	.129	1.62	1.18	6.95	4.29	.963	13.03	.728	1.67	33.3	95.1	50.5	53.1	.951
4c	.125	.129	1.62	1.17	6.99	4.31	.970	12.93	.722	1.68	33.0	97.2	52.1	52.6	.990
5a	.125	.129	1.62	1.34	7.46	4.60	.973	12.92	.827	1.33	37.0	77.0	45.9	47.9	.958
5b	.125	.129	1.61	1.35	7.52	4.67	.964	12.92	.839	1.31	37.3	75.9	46.8	49.2	.951
6a	.114	.121	2.75	1.09	9.86	3.59	.947	24.04	.396	3.95	40.0	66.1	45.5	47.0	.968
6b	.115	.118	2.75	1.10	10.01	3.64	.968	24.01	.400	3.87	40.3	64.9	45.5	47.2	.964
6c	.115	.121	2.74	1.11	9.93	3.62	.948	23.90	.405	3.90	40.0	66.0	46.3	47.2	.981
7a	.114	.121	2.75	1.38	11.98	4.36	.946	24.10	.502	3.07	45.5	51.1	42.2	43.2	.977
7b	.115	.118	2.75	1.40	11.99	4.36	.972	23.99	.509	2.94	46.2	49.4	41.5	42.4	.979
7c	.114	.121	2.76	1.39	11.99	4.34	.948	24.15	.504	3.05	45.7	50.6	42.8	43.5	.984
8	.114	.119	2.76	1.68	16.48	5.97	.955	24.21	.609	2.28	53.0	37.6	34.6	37.3	.928
9a	.116	.120	2.76	1.96	16.48	5.97	.965	23.83	.710	1.75	59.5	29.8	28.2	35.0	.806
9b	.116	.119	2.76	1.96	16.48	5.97	.972	23.81	.710	1.73	59.8	29.5	28.0	34.8	.805
10a	.117	.123	2.75	2.25	17.78	6.47	.953	23.51	.818	1.38	66.2	24.1	24.0	34.4	.698
10b	.116	.122	2.76	2.25	17.75	6.43	.956	23.72	.815	1.39	66.5	23.9	23.3	33.8	.689
10c	.116	.121	2.76	2.25	17.59	6.37	.959	23.69	.815	1.38	66.7	23.7	22.5	33.1	.680

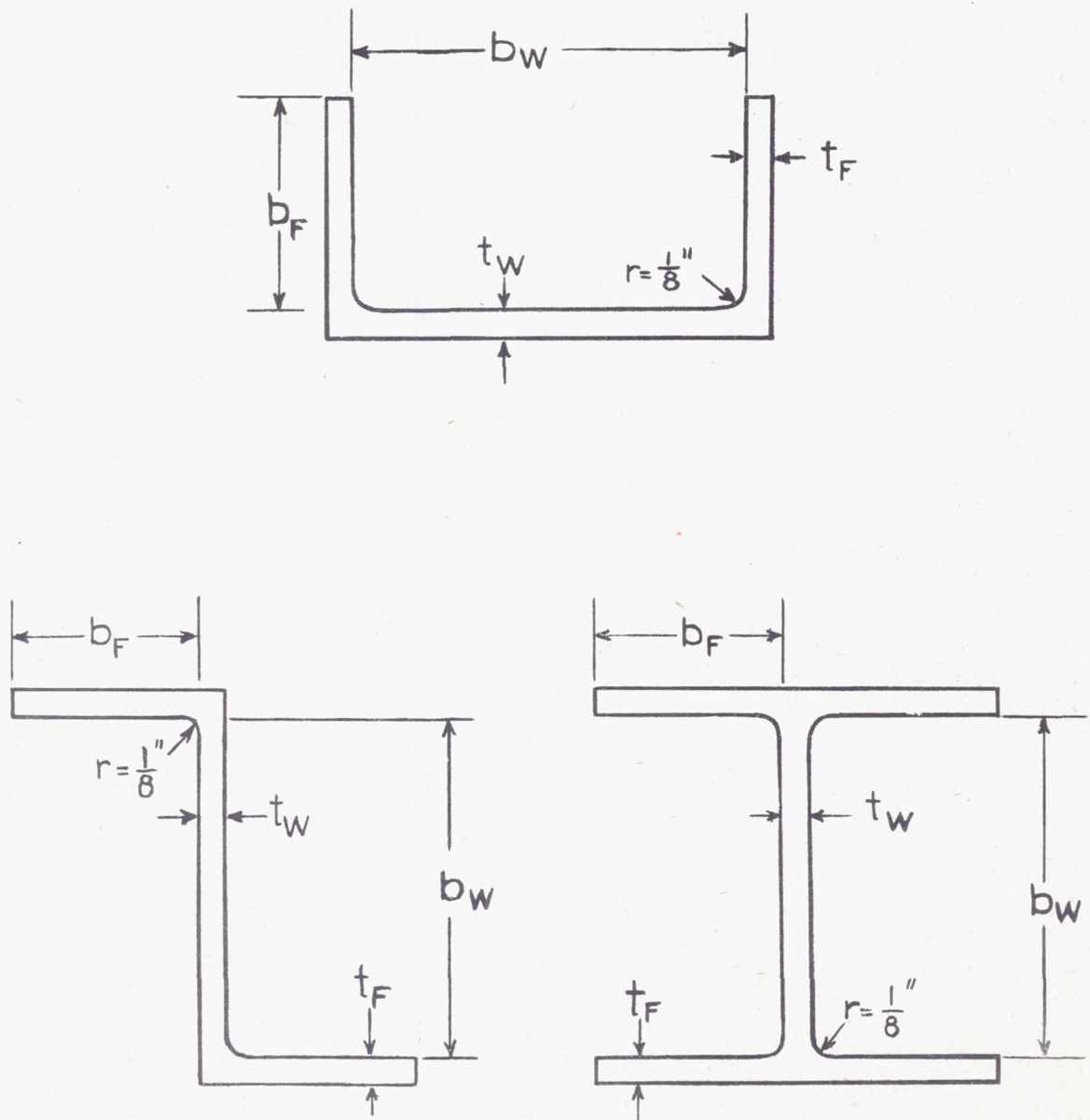
$$^a \sigma_{cr} = \frac{k_w n^2 E_c t_w^2}{12(1-\mu^2) b_w^2}, \text{ where } E_c = 10,700 \text{ ksi and } \mu = 0.3.$$

NATIONAL ADVISORY  
COMMITTEE FOR AERONAUTICS

TABLE 4.- DIMENSIONS OF COLUMNS AND TEST RESULTS  
FOR EXTRUDED 24S-T CHANNEL SECTIONS

Column	$t_w$ (in.)	$t_F$ (in.)	$b_w$ (in.)	$b_F$ (in.)	L (in.)	$\frac{L}{b_w}$	$\frac{t_w}{t_F}$	$\frac{b_w}{t_w}$	$\frac{b_F}{b_w}$	$k_w$ (fig. 3)	$\frac{b_w \sqrt{12(1-\mu^2)}}{t_w k_w}$	$\frac{\sigma_{cr}}{\eta}$ (ksi) (a)	$\sigma_{cr}$ (ksi)	$\bar{\sigma}_{max}$ (ksi)	$\frac{\sigma_{cr}}{\bar{\sigma}_{max}}$
1a	0.123	0.129	1.61	0.99	6.10	3.79	0.960	13.04	0.613	2.25	28.7	128.0	54.0	57.8	0.934
1b	.124	.128	1.61	.98	6.09	3.78	.967	12.99	.606	2.27	28.5	129.3	54.8	57.5	.953
2a	.123	.128	1.61	.99	6.50	4.04	.964	13.05	.613	2.25	28.7	127.8	56.1	56.5	.993
2b	.123	.128	1.60	.99	6.48	4.05	.959	13.01	.620	2.20	29.0	125.7	55.2	56.6	.975
3a	.125	.129	1.63	1.08	6.45	3.96	.971	13.03	.663	1.91	31.1	109.0	51.6	54.5	.947
3b	.125	.129	1.61	1.09	6.39	3.97	.966	12.91	.677	1.90	31.0	110.2	52.7	54.6	.965
3c	.125	.129	1.61	1.09	6.46	4.01	.966	12.91	.677	1.90	31.0	110.2	52.6	54.9	.958
3d	.124	.129	1.61	1.09	7.00	4.35	.966	12.93	.677	1.90	31.0	109.9	53.5	54.6	.980
4a	.124	.129	1.60	1.17	7.00	4.38	.962	12.90	.731	1.66	33.1	96.5	49.4	51.9	.952
4b	.125	.130	1.61	1.17	6.96	4.32	.961	12.91	.727	1.67	33.1	96.9	49.8	51.8	.961
4c	.125	.130	1.61	1.17	6.96	4.32	.963	12.83	.727	1.67	32.8	98.1	49.9	52.1	.958
4d	.125	.129	1.62	1.18	6.94	4.28	.964	13.00	.728	1.67	33.2	95.6	50.6	51.9	.975
4e	.124	.129	1.61	1.18	6.95	4.32	.960	12.95	.733	1.66	33.2	95.7	51.2	52.6	.973
4f	.125	.129	1.61	1.18	7.00	4.35	.965	12.90	.733	1.65	33.2	95.9	51.5	52.8	.975
5a	.125	.129	1.61	1.34	7.48	4.65	.963	12.92	.832	1.33	37.0	77.0	46.7	48.4	.965
5b	.125	.129	1.62	1.34	7.41	4.57	.963	13.00	.827	1.34	37.1	76.7	47.0	48.7	.965
5c	.124	.129	1.60	1.35	7.47	4.67	.962	12.86	.844	1.29	37.4	75.4	46.3	48.4	.957
6a	.115	.119	2.75	1.10	10.00	3.64	.964	23.87	.400	3.88	40.1	65.8	46.2	46.8	.987
6b	.114	.119	2.74	1.11	10.00	3.65	.959	23.99	.405	3.85	40.4	64.7	46.8	47.4	.987
6c	.114	.122	2.75	1.11	10.00	3.64	.939	24.03	.404	3.94	40.0	66.0	46.5	47.2	.985
7a	.114	.120	2.76	1.40	12.03	4.36	.954	24.14	.507	3.00	46.1	49.8	43.1	43.8	.984
7b	.115	.119	2.74	1.40	12.02	4.39	.966	23.85	.511	2.93	46.1	49.8	43.4	44.0	.986
7c	.114	.119	2.75	1.40	12.06	4.39	.957	24.09	.509	2.98	46.1	49.7	43.4	44.1	.984
8a	.125	.120	2.76	1.68	15.46	5.60	1.042	22.07	.609	2.10	50.3	42.5	37.5	38.9	.964
8b	.125	.120	2.76	1.68	15.44	5.59	1.042	22.11	.609	2.10	50.4	41.5	37.6	38.7	.972
8c	.125	.120	2.76	1.68	15.47	5.61	1.042	22.04	.609	2.10	50.3	41.8	37.9	38.9	.974
9a	.125	.120	2.75	1.96	16.30	5.93	1.039	21.97	.713	1.57	57.9	31.5	30.2	35.5	.851
9b	.125	.120	2.76	1.98	16.30	5.91	1.042	22.01	.717	1.54	58.5	30.7	30.1	35.7	.843
9c	.125	.121	2.76	1.97	16.30	5.91	1.041	21.99	.714	1.55	58.4	31.0	30.6	36.4	.841
10a	.126	.121	2.76	2.24	17.80	6.45	1.046	21.82	.812	1.27	64.0	25.8	24.0	34.0	.706
10b	.127	.121	2.76	2.23	17.85	6.47	1.047	21.72	.808	1.28	63.4	26.2	24.1	33.3	.724
10c	.126	.121	2.76	2.24	17.80	6.45	1.044	21.90	.812	1.27	64.2	25.6	23.5	35.6	.660

$$^a \sigma_{cr} = \frac{k_w \eta^2 E_c t_w^2}{\eta 12(1-\mu^2) b_w^2}, \text{ where } E_c = 10,700 \text{ ksi and } \mu = 0.3.$$



NATIONAL ADVISORY  
COMMITTEE FOR AERONAUTICS

Figure 1.- Cross sections of H-, Z-, and channel-section columns.

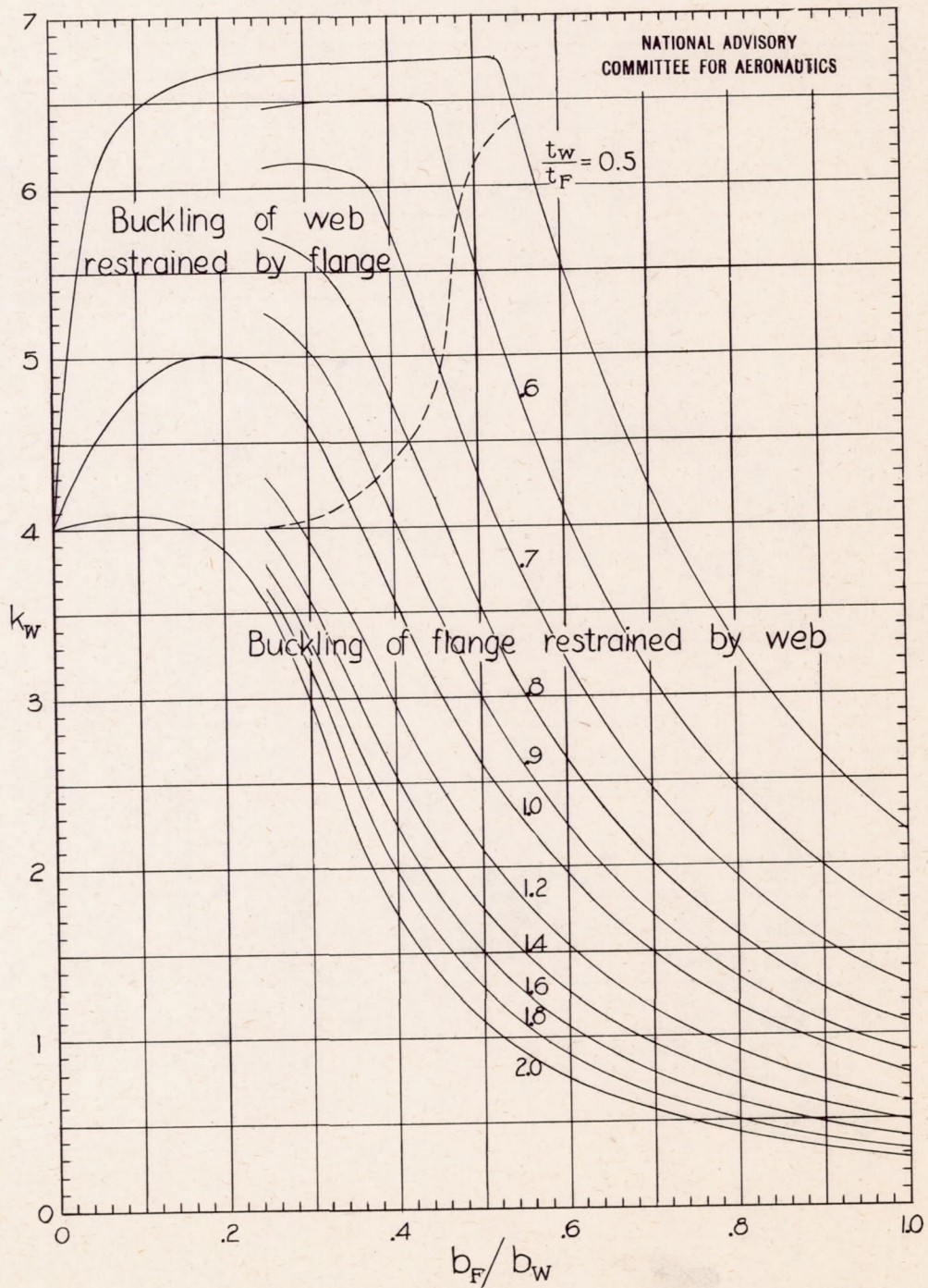


Figure 2.- Values of  $k_w$  for H-section columns. (From reference 4.)

$$\frac{\sigma_{cr}}{\eta} = \frac{k_w \pi^2 E_c t_w^2}{12(1-\mu^2) b_w^2}$$

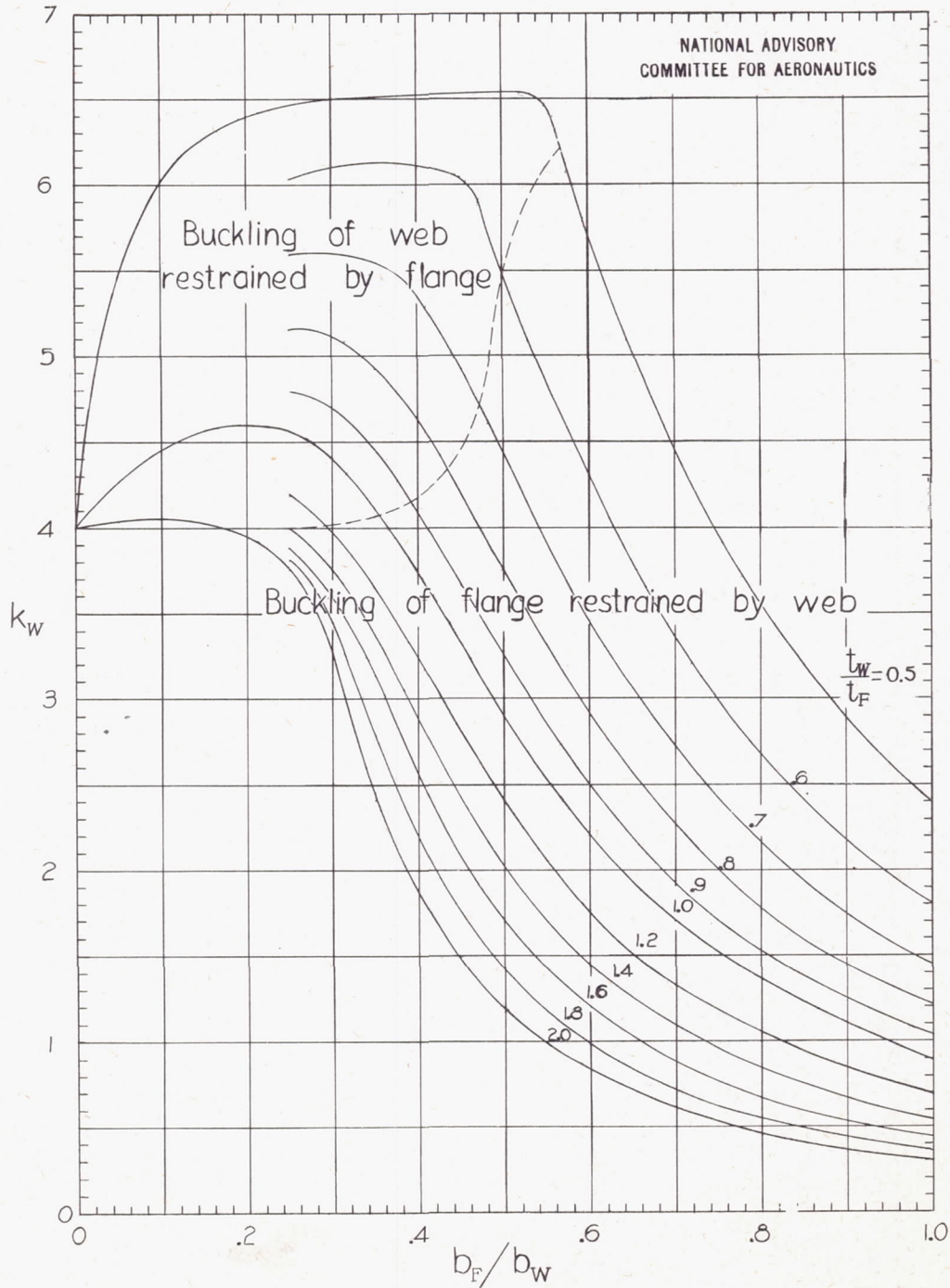


Figure 3.- Values of  $k_w$  for Z- and channel-section columns. (From reference 4.)

$$\frac{\sigma_{cr}}{\eta} = \frac{k_w \pi^2 E_c t_w^2}{12(1-\mu^2) b_w^2}$$

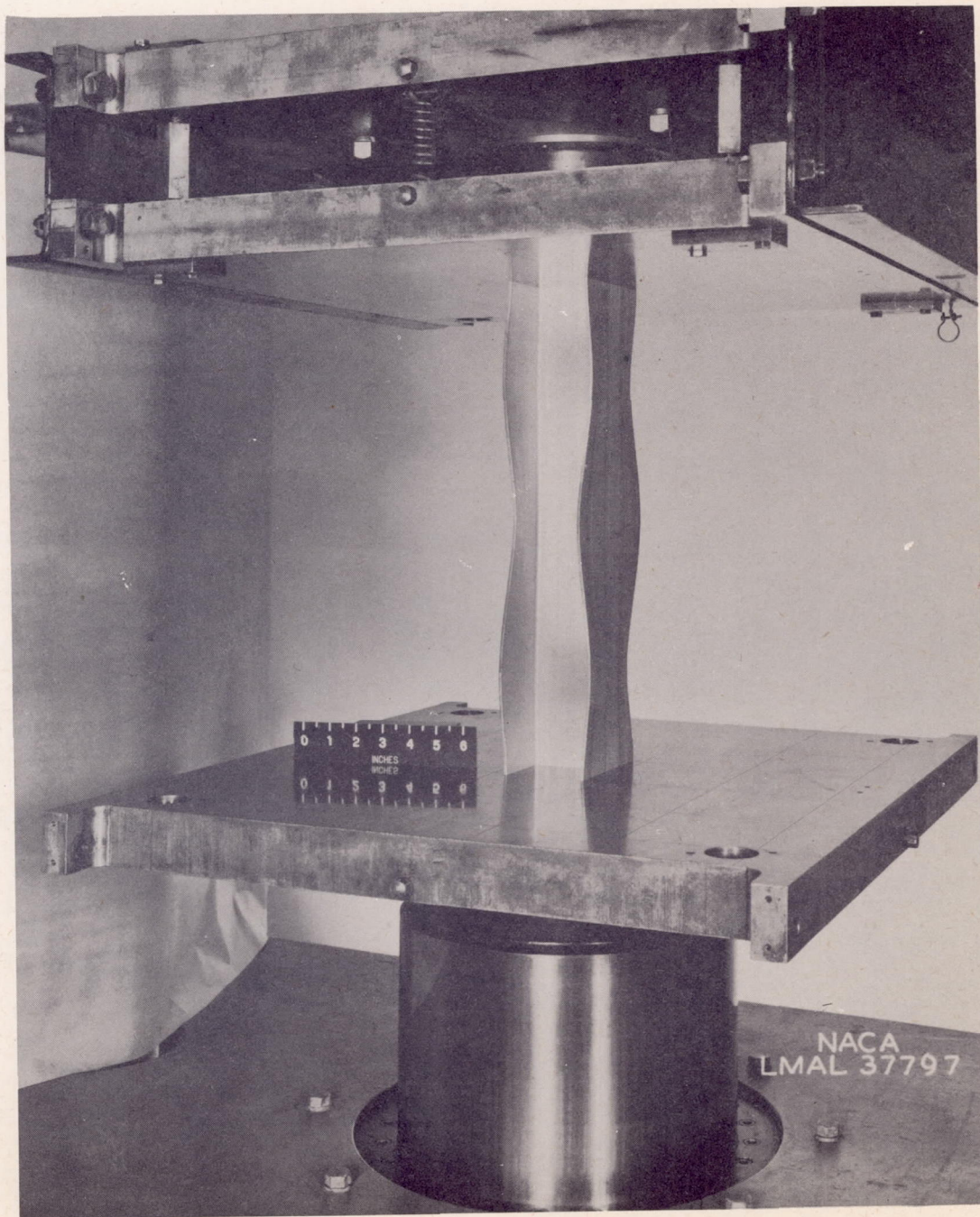


Figure 4.- Local instability of an H-section column.



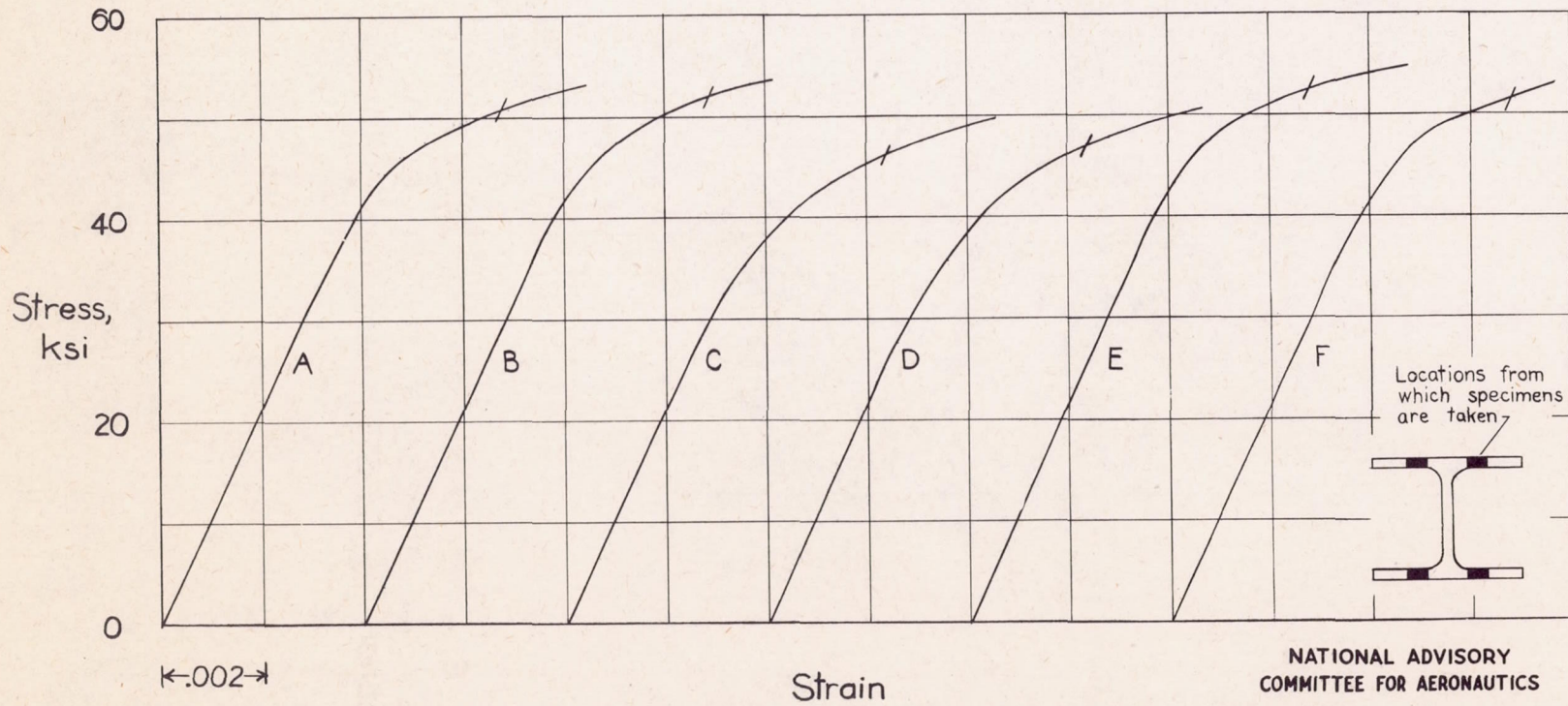
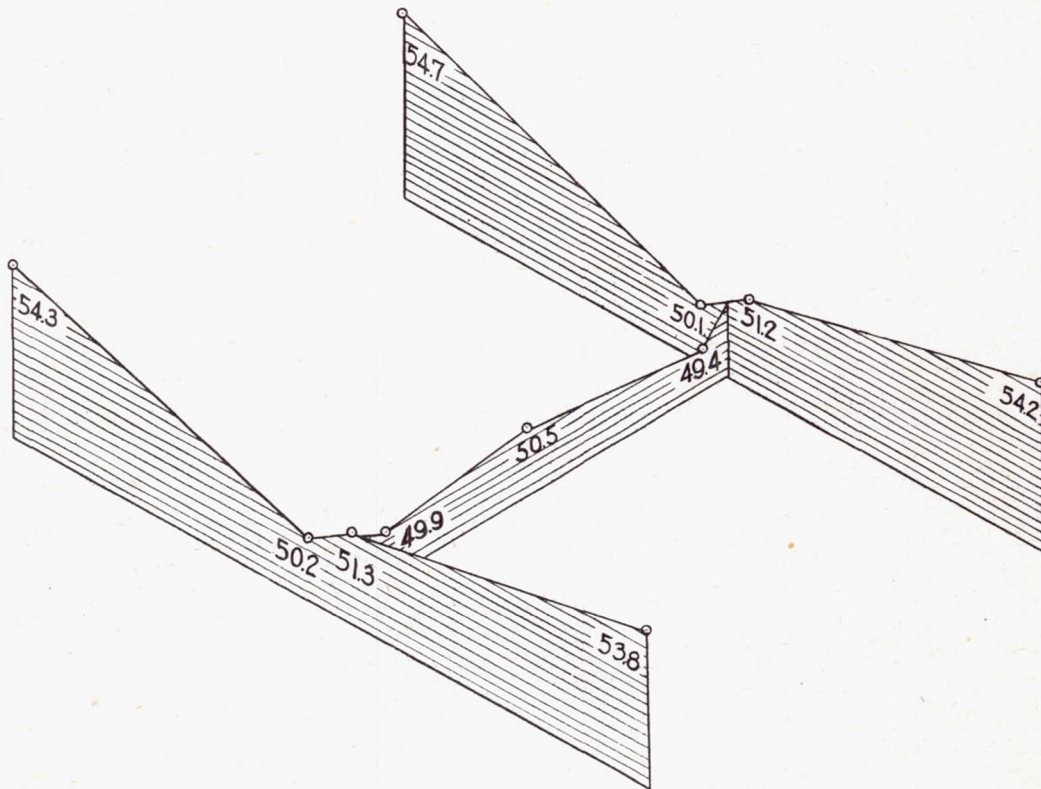


Figure 5.- Compressive stress-strain curves for extruded 24 S-T aluminum alloy.  
(Curves A, B, C, etc., are identified in table 1.)



NATIONAL ADVISORY  
COMMITTEE FOR AERONAUTICS

Figure 6. - Variation of the compressive yield stress over the cross section of an extruded H-section of 24S-T aluminum alloy. (Values in ksi)

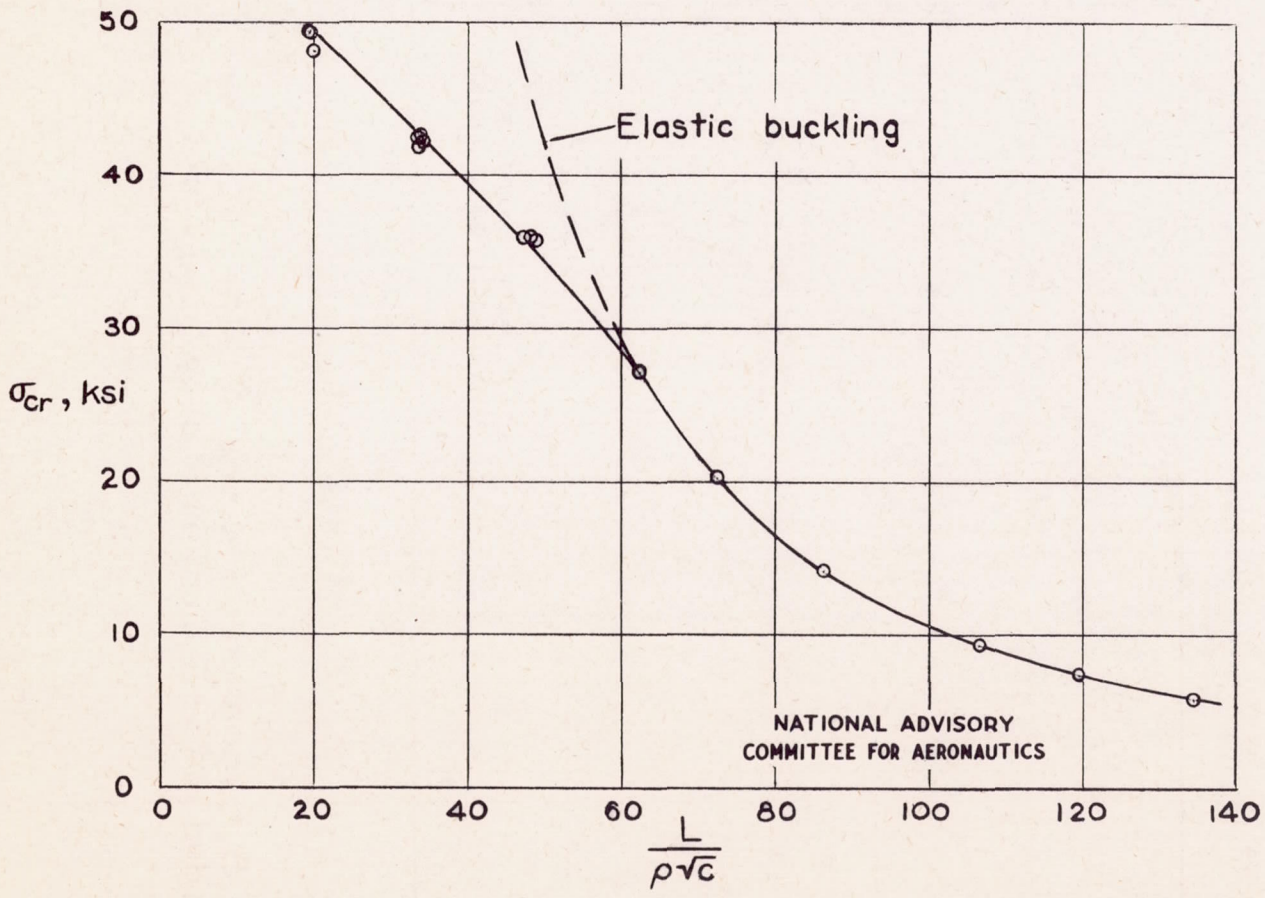


Figure 7.- Column curve for extruded 24S-T aluminum alloy.  $\sigma_{cy} = 50$  ksi.

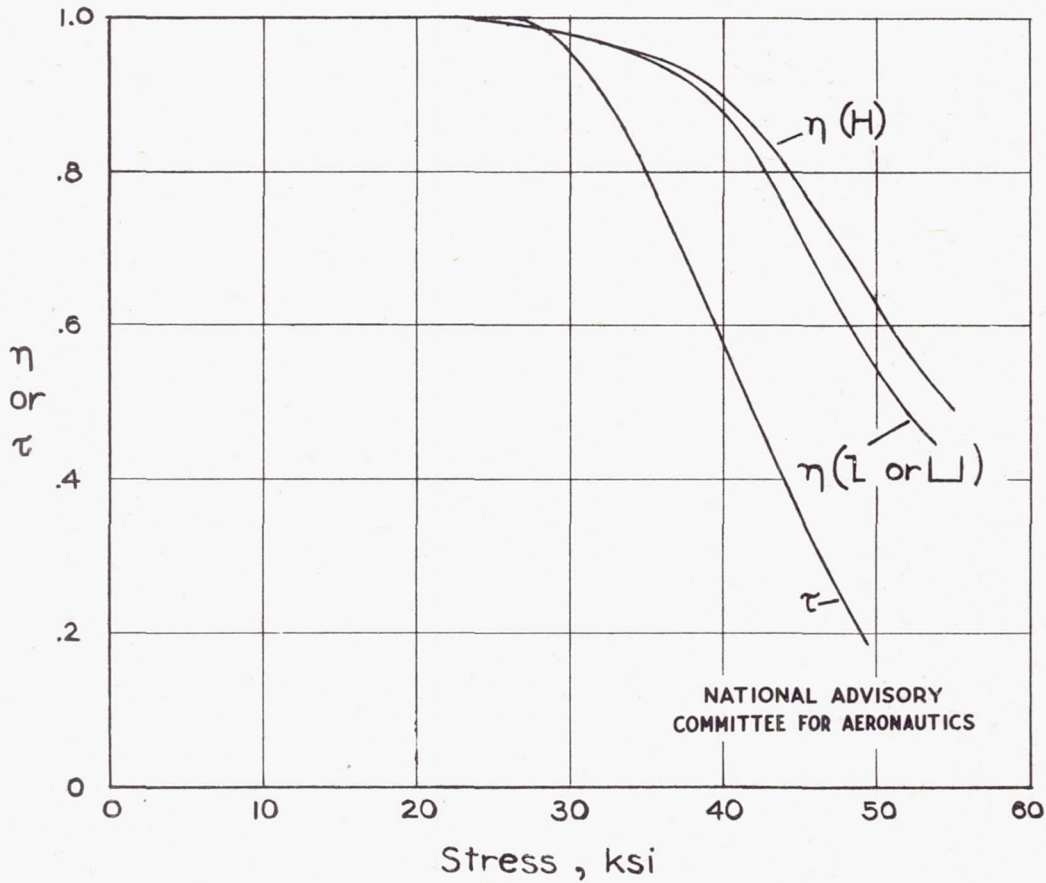


Figure 8.- Variation of  $\tau$  and  $\eta$  with stress for extruded 24S-T aluminum alloy.  $\sigma_{cy} = 50$  ksi.

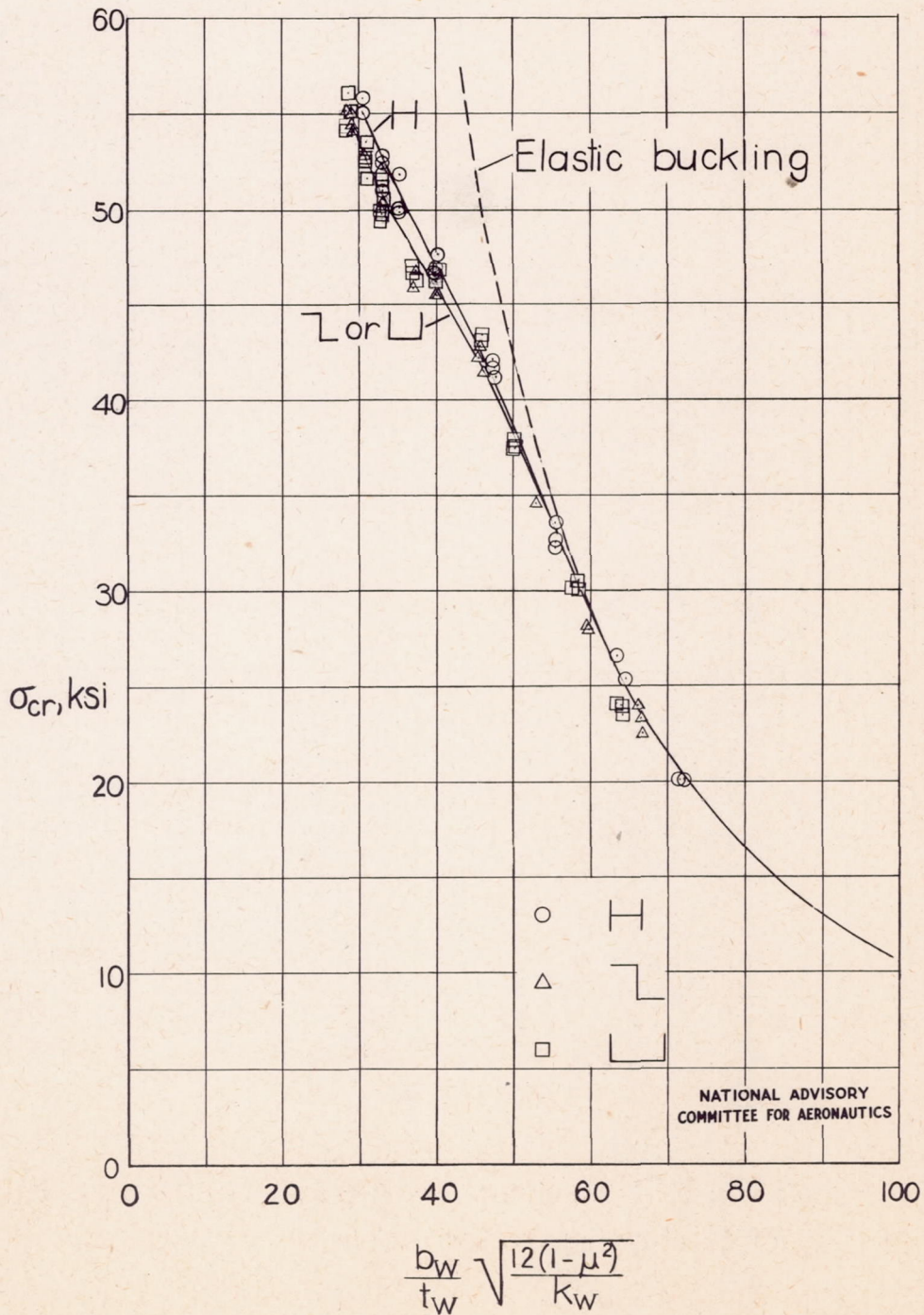


Figure 9. - Plate-buckling curves for extruded 24 S-T aluminum alloy obtained from tests of H-, Z-, and channel-section columns.  $\sigma_{cy} = 50$  ksi.

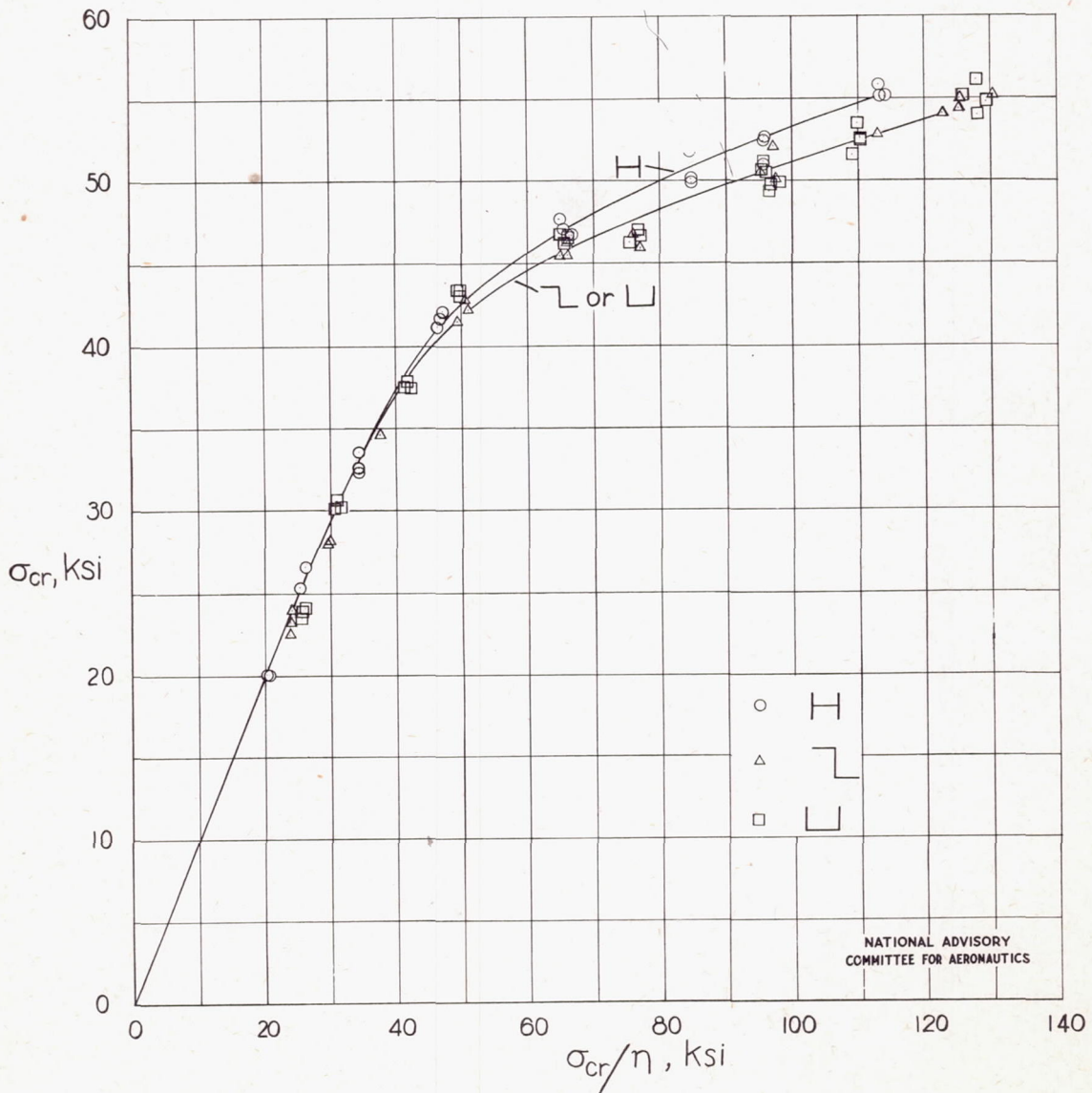


Figure 10.- Variation of  $\sigma_{cr}$  with  $\sigma_{cr}/\eta$  for plates of extruded 24S-T aluminum alloy obtained from tests of H-, Z-, and channel-section columns.  $\sigma_{cy} = 50$  ksi.

NATIONAL ADVISORY  
COMMITTEE FOR AERONAUTICS

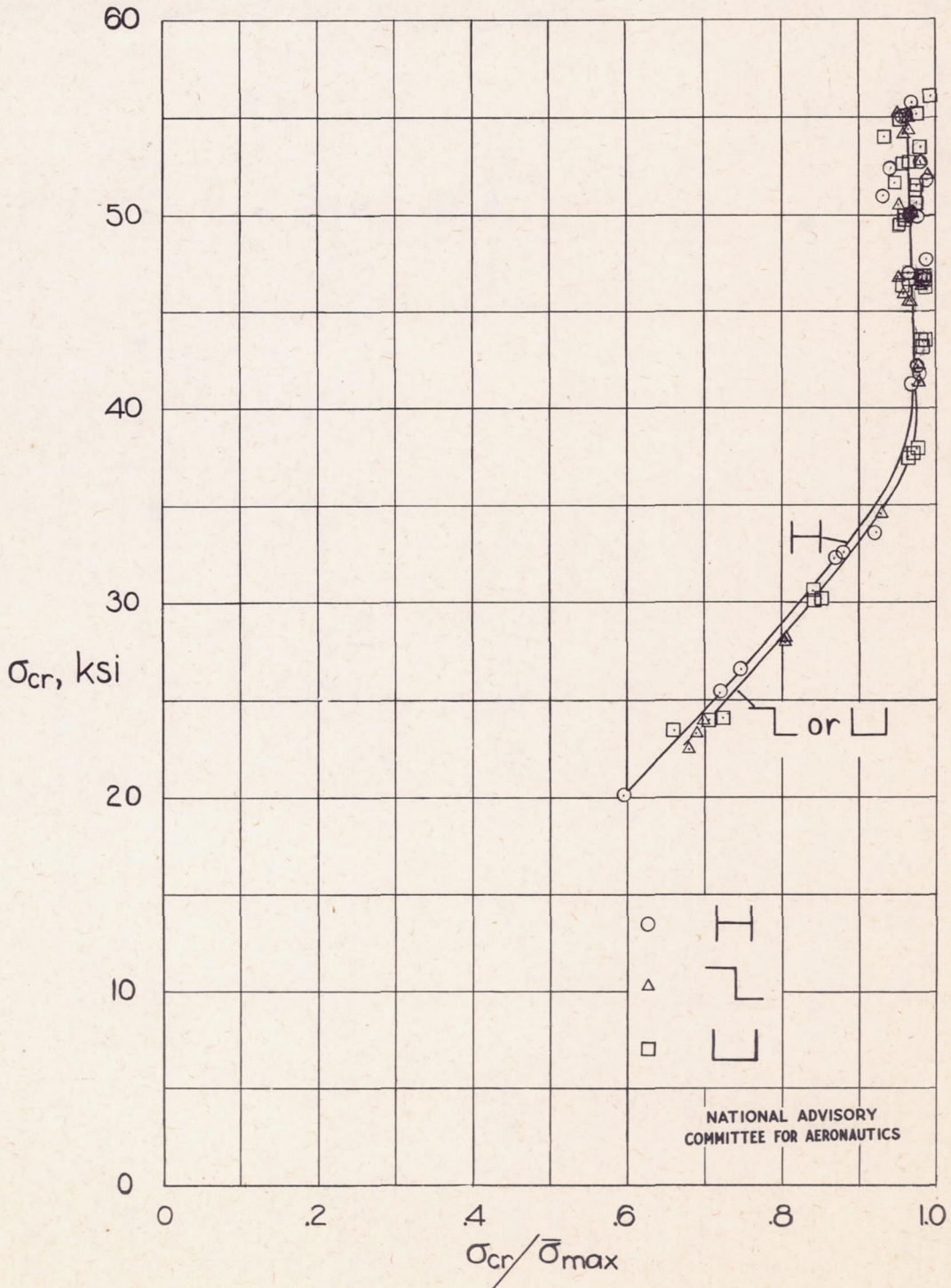


Figure 11. - Variation of  $\sigma_{cr}$  with  $\sigma_{cr}/\bar{\sigma}_{max}$  for extruded 24S-T aluminum - alloy H-, Z-, and channel-section columns.  $\sigma_{cy} = 50$  ksi.

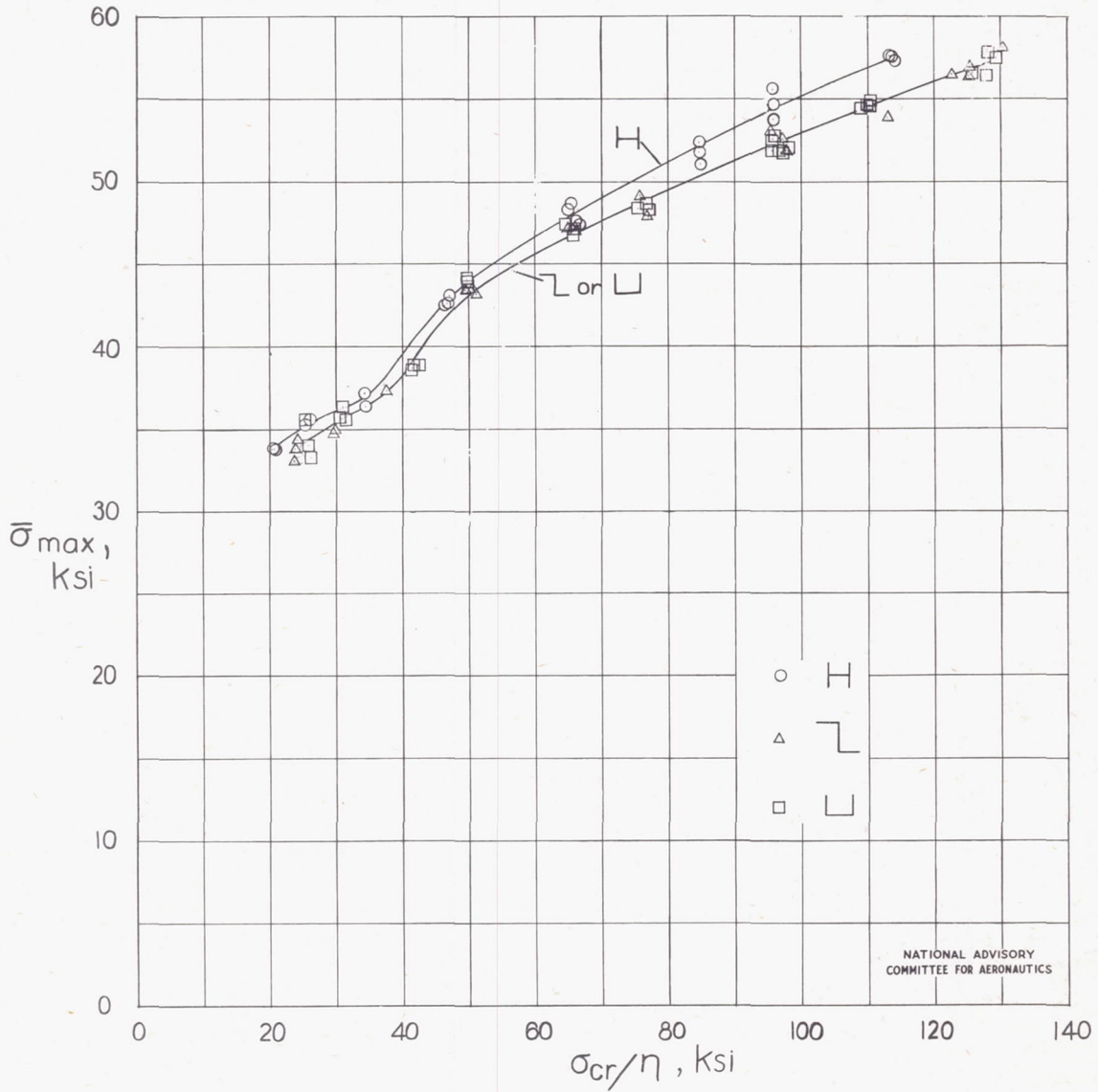


Figure 12.- Variation of  $\bar{\sigma}_{max}$  with  $\sigma_{cr}/\eta$  for extruded 24 S-T aluminum - alloy H-, Z-, and channel-section columns.  $\sigma_{cy} = 50$  ksi.